AD-A046 689 NAVAL UNDERWATER SYSTEMS CENTER NEWPORT R I F/G 17/1

SPATIAL COHERENCE OF A SIGNAL REFLECTED FROM A TIME-VARYING RAN--ETC(U)

FEB 71 B F CRON

UNCLASSIFIED NUSC-TM-TA11-46-71 NL

| OF |

AD A046689

END

DATE FILMED

12-77

DDC

MOST Project -3

Copy to___

Copy No. 2

Project Number
1-B-055-00-00
ZR 011 01 01

NAVAL UNDERWATER SYSTEMS CENTER
NEWPORT, RHODE ISLAND 02840

SPATIAL COHERENCE OF A SIGNAL REFLECTED FROM A TIME-VARYING RANDOM SURFACE.

by

Benjamin F. Cron

ZRØ11Ø1Ø1

Technical Memorandum No. NUSC-TM-TA11-46-71

23 Feb 1971

22p.

ABSTRACT

The coherence between two points of the received acoustic waveform after reflection from a time varying random surface is evaluated for the far field case. A Neumann-Pierson spectrum and an isotropic sea is considered. For the low roughness case, the coherence is computed for wind speeds from 2 to 10 knots. For the specular and non-specular direction, the coherent region is on the order of the pattern resulting from the insonified surface area.

ADMINISTRATIVE INFORMATION

This memoradnum was prepared under NUSC/NL Project Title: Acoustic Statistical Applications to Sonar System Design, B. F. Cron, Principal Investigator. The Sponsoring Activity was Chief of Naval Material, J. B. Huth, Program Manager.

406 068

Tech Memo
No. TA 11-46-71

INTRODUCTION

A very important problem in underwater sound detection is the computation of array gain. The earliest calculation of array gain assumed that the signal was perfectly coherent and that the noise between receivers was perfectly incoherent. Thus, the signal added as N^2 and the noise as N, where N is the number of elements in the array. The array gain is 10 log N for this idealized situation. Later work assumed that the noise was isotropic, that is the same in all directions. For this case, the noise was incoherent at half wave length spacing and almost incoherent when spacing between elements is greater than 2 wavelengths. This model was later extended to the case of directional noise which showed that the array gain was very dependent on steering direction.

In comparison with the noise models, relatively little work has been done on signal coherence. A notable exception to this is the excellent work by Parkins[1]. In this memorandum a generalization and correction of the work by Parkins on small roughness is made. In addition, plots of coherence are provided. The purpose of this memorandum is to provide a model and computations for some typical cases, for the coherence of a signal reflected from the ocean surface.

REFLECTED PRESSURE

We will consider a single frequency waveform, exp ($i2\pi ft$) insonifying a finite area of ocean surface. The reflected pressure in the far field is

$$p_i(t) = -\frac{iB}{\lambda R_i} \exp\left[i(2\pi f t - k R_i)\right] \qquad \#1$$

$$\cdot \iint_{-\infty}^{\infty} dx_i\, dy_i\, \hat{p}(x_i, y_i) \exp\left[ik\left(a_i x_i + b_i y_i + c_i \zeta_i(x_i, y_i, t)\right)\right]$$

An equation similar to equation #1 was utilized by Eckart[2]. A discussion of equation #1 and the corresponding assumptions involved for the rough surface case are given by Nuttall and Cron[3]. In equation #1, $P_i(t)$ is the reflected complex pressure at the i^{th} point at time t. B is a geometric factor, λ is the acoustic wavelength, R_i is the distance from surface origin to the i^{th} point, k is the wave number,

$\hat{P}(x_i, y_i)$ is the insonified pressure on the surface at x_i, y_i; a_i, b_i and c_i are the sum of the direction cosines of the incident and reflected pressures for the x, y and z directions, respectively. $\zeta(x_i, y_i, t)$ is the surface height at the point x_i, y_i at time t. The incident mathematical signal, exp ($i2\pi ft$), has positive frequencies only. This signal is modulated by the time varying ocean surface. Since this time variation is slow in comparison to the variation of exp ($i2\pi ft$), then $P_i(t)$ is narrow band. This $P_i(t)$ contains only positive frequencies. $P_i(t)$ is an analytic signal. The real part of $P_i(t)$ is the actual pressure and the imaginary part of $P_i(t)$ is the Hilbert transform of the real part.

MUTUAL AND COMPLEX DEGREE OF COHERENCE

We now consider two points of the pressure field. (See Figure 1)

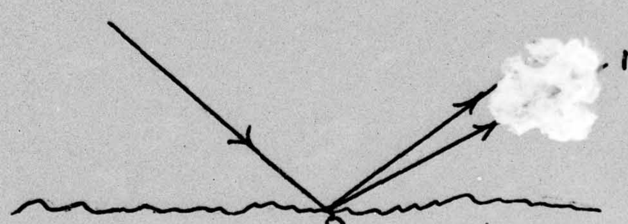

Fig. 1

The mutual coherence function $\Gamma_{12}(\tau)$, as defined by Born and Wolf[4] is

$$\Gamma_{12}(\tau) = \langle p_1(t)\, p_2^*(t-\tau) \rangle \qquad \#2$$

Where * is the complex conjugate operator
< > is the ensemble average
τ is the time delay between points 1 and 2

The complex degree of coherence is defined as

$$\gamma_{12}(\tau) = \frac{\Gamma_{12}(\tau)}{\sqrt{\Gamma_{11}(0)\,\Gamma_{22}(0)}} \qquad \#3$$

By the use of Schwartz's inequality, it can be shown that

$$0 \leq |\gamma_{12}(\tau)| \leq 1$$

The upper limit corresponds to a perfect coherence of the pressures at points 1 and 2, whereas the lower limit signifies perfect incoherence between the points at 1 and 2. In signal processing terminology, $\Gamma_{12}(\tau)$ is called the complex correlation of $p_1(t)$ and $p_2(t)$. It can be shown that

$$\Gamma_{12}(\tau) = 2\left[R_p(\tau) + i R_p^H(\tau)\right] \qquad \#4$$

where $$R_p(\tau) = \langle Re\left(p_1(t)\right) Re\left(p_2(t-\tau)\right)\rangle$$

and $$R_p^H(\tau) = \langle Re\left(p_1(t)\right) Im\left(p_2(t-\tau)\right)\rangle$$

Where Re and Im signify the real and imaginary parts, respectively. Thus, from equation 4, the correlation of two signals at points 1 and 2 may be obtained, since

$$R_p(\tau) = \frac{1}{2} Re\left(\Gamma_{12}(\tau)\right)$$

MUTUAL COHERENCE FUNCTION FOR A TIME VARYING SURFACE

From equation #1 and referring to Fig. 1,

$$p_1(t)\, p_2^*(t-\tau) = \exp(i2\pi f\tau)\exp(-ik(R_1-R_2))\, B^2/\lambda^2 R_1 R_2$$
$$\cdot \iiiint_{-\infty}^{\infty} dx_1\, dy_1\, dx_2\, dy_2\, \hat{p}(x_1, y_1)\, \hat{p}(x_2, y_2) \qquad \#5$$
$$\cdot \exp\left[ik(a_1 x_1 - a_2 x_2 + b_1 y_1 - b_2 y_2 + c_1 \zeta_1 - c_2 \zeta_2)\right]$$

In order to keep the symbols to a minimum, we will set $\tau = 0$, and
$K = \exp\left[-ik(R_1 - R_2)\right] \frac{B^2}{\lambda^2 R_1 R_2}$
We now take the ensemble average of $\langle p_1(t)\, p_2^*(t)\rangle$ and we will drop the t's. Then

$$\langle p_1 p_2^* \rangle = K \iiiint_{-\infty}^{\infty} dx_1\, dy_1\, dx_2\, dy_2\, \hat{p}(x_1, y_1)\, \hat{p}(x_2, y_2) \qquad \#6$$

$$\cdot \exp[ik(a_1 x_1 - a_2 x_2 + b_1 y_1 - b_2 y_2)] \langle \exp[ik(c_1 \zeta_1 - c_2 \zeta_2)] \rangle$$

We will assume that the surface height is Gaussian distributed. Kinsman[5] cites experimental data showing that the surface height is very close to a Gaussian distribution.

$$\langle \exp[ik(c_1 \zeta_1 - c_2 \zeta_2)] \rangle = \iint_{-\infty}^{\infty} d\zeta_1\, d\zeta_2\, \exp[ik(c_1 \zeta_1 - c_2 \zeta_2)]\, p(\zeta_1, \zeta_2)$$

and for a joint Gaussian $p(\zeta_1, \zeta_2)$ this becomes

$$\langle \exp[ik(c_1 \zeta_1 - c_2 \zeta_2)] \rangle = \exp\left[-\frac{k^2 \sigma^2}{2}(c_1^2 + c_2^2 - 2 c_1 c_2 \rho)\right] \qquad \#7$$

where

$$\rho = \rho(x_1 - x_2,\ y_1 - y_2,\ t_1 - t_2)$$

substituting 7 into equation 6, we obtain

$$\langle p_1 p_2^* \rangle = K \iiiint_{-\infty}^{\infty} dx_1\, dy_1\, dx_2\, dy_2\, \hat{p}(x_1, y_1)\, \hat{p}(x_2, y_2) \qquad \#8$$

$$\exp[ik(a_1 x_1 - a_2 x_2 + b_1 y_1 - b_2 y_2)] \exp\left[-\frac{k^2 \sigma^2}{2}(c_1^2 + c_2^2)\right] \exp[k^2 \sigma^2 c_1 c_2 \rho]$$

SMALL ROUGHNESS CASE

In this section, we consider the small acoustic roughness case. For this case we can expand the term $\exp[k^2 \sigma^2 c_1 c_2 \rho]$ in equation #8 as

$$\exp[k^2 \sigma^2 c_1 c_2 \rho] \cong 1 + k^2 \sigma^2 c_1 c_2 \rho \qquad \#9$$

Since $\rho \leq 1$, this expansion is sufficiently accurate if $k^2 \sigma^2 c_1 c_2 \ll 1$. Substituting equation #9 into equation #8, the first term of equation #9 results in a coherent component and the second term results in an incoherent component.

The first term called the coherent component is

$$\langle f_1 f_2^* \rangle_{COH} = K \exp\left[-\frac{k^2\sigma^2}{2}(c_1^2+c_2^2)\right] \qquad \#10$$

$$\cdot \iiiint_{-\infty}^{\infty} dx_1\, dy_1\, dx_2\, dy_2\; \hat{f}(x_1,y_1)\, \hat{f}(x_2,y_2)$$

$$\cdot \exp\left[ik(a_1x_1 - a_2x_2 + b_1y_1 - b_2y_2)\right]$$

The incoherent term is

$$\langle f_1 f_2^* \rangle_{IN} = K \exp\left[-\frac{k^2\sigma^2}{2}(c_1^2+c_2^2)\right] \qquad \#11$$

$$\cdot \iiiint_{-\infty}^{\infty} k^2\sigma^2 c_1 c_2\, \rho\, \hat{f}(x_1,y_1)\, \hat{f}(x_2,y_2) \exp\left[ik(a_1x_1 - a_2x_2 + b_1y_1 - b_2y_2)\right]$$

The coherent component in equation #10 can be integrated for some values of $\hat{f}(x,y)$. In this study, it will be integrated for Gaussian insonification. The incoherent component is more difficult.

Let us now consider equation #11. We will assume that the properties of the surface depend only on the difference of the coordinates.

Let $u = x_1 - x_2$

$v = y_1 - y_2$

then $\langle f_1 f_2^* \rangle_{IN} = K \exp\left[-\frac{k^2\sigma^2}{2}(c_1^2+c_2^2)\right] k^2\sigma^2 c_1 c_2\, \rho(u,v,0)$

$$\cdot \iiiint_{-\infty}^{\infty} du\, dv\, dx_2\, dy_2\; \hat{f}(x_2+u,\, y_2+v)\, \hat{f}(x_2,y_2)$$

$$\cdot \exp\left[ik(a_1(x_2+u) - a_2x_2 + b_1(y_2+v) - b_2y_2)\right]$$

Let $\alpha = x_2 + u/2$

$\beta = y_2 + v/2$

then

$$\langle f_1 f_2^* \rangle_{IN} = K \exp\left[-\frac{k^2\sigma^2}{2}(c_1^2+c_2^2)\right] k^2\sigma^2 c_1 c_2\, \rho(u,v,0)$$

$$\cdot \iiiint_{-\infty}^{\infty} d\alpha\, d\beta\, du\, dv\ \hat{f}\left(\alpha+\frac{u}{2}, \beta+\frac{v}{2}\right) \hat{f}\left(\alpha-\frac{u}{2}, \beta-\frac{v}{2}\right) \qquad \#12$$

$$\cdot \exp\left[ik\left\{a_1\left(\alpha+\frac{u}{2}\right) - a_2\left(\alpha-\frac{u}{2}\right) + b_1\left(\beta+\frac{v}{2}\right) - b_2\left(\beta-\frac{v}{2}\right)\right\}\right]$$

We now assume that the effective extents on the surface of the incident illumination $\hat{f}$ are much larger than the distances at which the surface heights are statistically dependent on each other. That is, the correlation distance is much less than the insonification distance. Using this fact, we may approximate equation #12 by

$$\langle p_1 p_2^* \rangle_{IN} = K \exp\left[-\frac{k^2\sigma^2}{2}(c_1^2+c_2^2)\right] \qquad \#13$$

$$\cdot \iint_{-\infty}^{\infty} du\, dv\, \rho(u,v,0) \exp\left\{ik\left[\left(\frac{a_1+a_2}{2}\right)u + \left(\frac{b_1+b_2}{2}\right)v\right]\right\}$$

$$\cdot \iint_{-\infty}^{\infty} d\alpha\, d\beta\, \hat{f}^2(\alpha,\beta) \exp\left\{ik\left[(a_1-a_2)\alpha + (b_1-b_2)\beta\right]\right\}$$

Equation #13 is a generalization and correction of Parkin's work. Equation #13 is symmetric with respect to points 1 and 2, whereas Parkin's results are non-symmetric. For the case of Gaussian insonification, Parkin's equations result in incorrect coherence values.

Thus for the incoherent component, a four fold integral has been approximated by the product of two double integrals. Equations #10 and #13 are the general equations for the coherent and incoherent components.

GAUSSIAN INSONIFICATION AND NEUMANN-PIERSON SPECTRUM

We will now obtain the equations for the special cases of Gaussian surface insonification and a Neumann-Pierson height spectrum. Let the surface Gaussian insonification be

$$\hat{f}(x_1, y_1) = \exp\left[-\frac{(x_1^2+y_1^2)}{2L^2}\right]$$

Thus the insonified pressure is 1 at the origin and falls to a value of $1/\sqrt{e}$ at a distance of L units from the origin.

Let us consider the integral

$$I_1 = \int_{-\infty}^{\infty} dx_1 \exp\left(-\frac{x_1^2}{2L^2}\right) \exp(ika_1x_1)$$

Completing squares or using the analogy of the characteristic function of a Gaussian distribution, we obtain

$$I_1 = \sqrt{2\pi L^2}\, \exp\left(-\frac{k^2a_1^2L^2}{2}\right) \qquad \#14$$

Thus for equation #10, we have

$$\langle f_1 f_2^* \rangle_{COH} = K^2(2\pi L^2)^2 \exp\left[-\frac{k^2L^2}{2}\left(a_1^2+a_2^2+b_1^2+b_2^2\right)\right] \qquad \#15$$

Let us now consider the second double integral in equation #13. This integral is

$$I_2 = \iint_{-\infty}^{\infty} d\alpha\, d\beta\, \hat{f}^2(\alpha,\beta) \exp\left\{ik\left[(a_1-a_2)\alpha + (b_1-b_2)\beta\right]\right\}$$

Again

$$\hat{f}(\alpha,\beta) = \exp\left[-\frac{(\alpha^2+\beta^2)}{2L^2}\right]$$

Using the results as given in equation #14, we obtain

$$I_2 = \pi L^2 \exp\left[-\frac{k^2(a_1-a_2)^2L^2}{2}\right] \exp\left[-\frac{k^2(b_1-b_2)^2L^2}{2}\right] \qquad \#16$$

Let us now consider the first double integral of equation #13.

$$I_3 = \iint_{-\infty}^{\infty} \rho(u,v,0) \exp\left\{ik\left[\left(\frac{a_1+a_2}{2}\right)u + \left(\frac{b_1+b_2}{2}\right)v\right]\right\} du\, dv$$

For brevity purposes, let

$$\bar{a} = \frac{a_1+a_2}{2}, \quad \bar{b} = \frac{b_1+b_2}{2}$$

We now express surface spatial correlation $\rho(u,v,0)$ in terms of the directional wave spectrum $\hat{A}^2(k_x,k_y)$. K_x and K_y are the surface wave numbers in rectangular coordinates. From Kinsman[5]

$$\sigma^2 \rho(u,v,0) = \iint_{-\infty}^{\infty} dk_x\, dk_y\, \hat{A}^2(k_x,k_y) \cos(k_x u + k_y v)$$

Thus

$$I_3 = \iint_{-\infty}^{\infty} du\, dv \exp\left[ik(\bar{a}u + \bar{b}v)\right]$$
$$\cdot \iint_{-\infty}^{\infty} \frac{dk_x\, dk_y}{\sigma^2} \hat{A}^2(k_x,k_y) \cos(k_x u + k_y v)$$

Let

$$\cos(k_x u + k_y v) = \frac{\exp[i(k_x u + k_y v)] + \exp[-i(k_x u + k_y v)]}{2}$$

then

$$I_3 = \iint_{-\infty}^{\infty} dk_x\, dk_y \frac{\hat{A}^2(k_x,k_y)}{2\sigma^2}$$
$$\cdot \iint_{-\infty}^{\infty} du\, dv \Big[\exp\left\{i\left[(k\bar{a} + k_x)u + (k\bar{b} + k_y)v\right]\right\}$$
$$+ \exp\left\{i\left[(k\bar{a} - k_x)u + (k\bar{b} - k_y)v\right]\right\}\Big]$$

Integrating over u and v and using the relation

$$\int_{-\infty}^{\infty} \exp(i\alpha u)\, du = 2\pi\, \delta(\alpha)$$

where $\delta(\alpha)$ is the Kronecker delta, we obtain

$$I_3 = \iint_{-\infty}^{\infty} dk_x\, dk_y\, \hat{A}^2(k_x,k_y)(2\pi)^2 \Big[\delta(\bar{a}k + k_x)\,\delta(\bar{b}k + k_y)$$
$$+ \delta(\bar{a}k - k_x)\,\delta(k\bar{b} - k_y)\Big]$$

Integrating on K_x and K_y, we obtain

$$I_3 = \frac{2\pi^2}{\sigma^2}\left\{\hat{A}^2(-\bar{a}k, -\bar{b}k) + \hat{A}^2(\bar{a}k, \bar{b}k)\right\} \qquad \#17$$

In order to obtain some numerical values of coherence, we will assume an isotropic sea, that is waves equally likely in all directions. To obtain this, let us first state the relation between the directional wave spectrum in rectangular and polar coordinates.

Then, (See Kinsman).

$$\hat{A}^2(k_x, k_y) = \frac{\sqrt{g}\, A^2\left(\sqrt{g}\,(k_x^2 + k_y^2)^{1/4},\ \tan^{-1}\left(\frac{k_y}{k_x}\right)\right)}{(k_x^2 + k_y^2)^{3/4}}$$

Then

$$I_3 = \frac{2\pi^2}{\sigma^2}\,\frac{\sqrt{g}}{2\,k^{3/2}\,(\bar{a}^2 + \bar{b}^2)^{3/4}}$$

$$\cdot \left\{ A^2\left[\sqrt{gk}\,(\bar{a}^2 + \bar{b}^2)^{1/4},\ \tan^{-1}\left(\frac{-b}{-a}\right)\right] + A^2\left[\sqrt{gk}\,(\bar{a}^2 + \bar{b}^2)^{1/4},\ \tan^{-1}\left(\frac{b}{a}\right)\right]\right\}$$

For an isotropic surface $A^2(\omega, \theta) = \dfrac{A_1^2(\omega)}{2\pi}$

and

$$I_3 = \frac{2\pi^2\sqrt{g}}{2\pi\,(k)^{3/2}\,\sigma^2}\left\{\frac{A_1^2\left(\sqrt{gk}\,(\bar{a}^2 + \bar{b}^2)^{1/4}\right)}{(\bar{a}^2 + \bar{b}^2)^{3/4}}\right\} \qquad \#18$$

Thus, we have evaluated I_3 for a general directional wave spectrum (equation #17) and for an isotropic sea (equation #18).

For the Neumann-Pierson spectrum

$$A_1^2(\omega) = \frac{\pi}{2}\,\frac{C}{\omega^6}\exp\left[-\frac{2g^2}{\omega^2 s^2}\right] \qquad \#19$$

where g is the acceleration of gravity
s is the wind speed.

EQUATIONS FOR COMPUTATION

For the reader's convenience, let us now collect the equations needed for computation. As stated previously, for Gaussian insonification and an isotropic sea with a Neumann-Pierson spectrum at a point

$$\langle f_1 f_2^* \rangle_{COH} = K_1 (2\pi L^2)^2 \exp\left[-\frac{k^2 L^2}{2}(a_1^2 + b_1^2 + a_2^2 + b_2^2)\right] \qquad \#20$$

$$\langle f_1 f_2^* \rangle_{IN} = K_1 \pi L^2 \exp\left[-\frac{k^2 (a_1 - a_2)^2 L^2}{4}\right] \exp\left[-\frac{k^2 (b_1 - b_2)^2 L^2}{4}\right]$$

$$\cdot \frac{2\pi^2 \sqrt{g}}{2\pi k^{3/2}} \left[\frac{A_1^2 (\sqrt{gk}(\bar{a}^2 + \bar{b}^2)^{1/4})}{\sigma^2 (\bar{a}^2 + \bar{b}^2)^{3/4}}\right] k^2 \sigma^2 c_1 c_2 \qquad \#21$$

where

$$K_1 = \frac{B^2}{\lambda^2 R_1 R_2} \exp(i 2\pi f \tau) \exp[-ik(R_1 - R_2)] \exp\left[-\frac{k^2 \sigma^2}{2}(c_1^2 + c_2^2)\right].$$

The other terms have been defined previously

$$A_1^2(\omega) = \frac{\pi}{2} \frac{c}{\omega^6} \exp\left(-\frac{2g^2}{\omega^2 s^2}\right) \qquad \#22$$

Let $\tau = 0$ and consider points 1 and 2 to lie on a circle with the center at the origin, so that $R_1 = R_2$.

In the cgs system g=980.665 cm. If s is expressed in knots, then to change to cm/sec., we must multiply by 185,200/3600. In equation #22, c=30,500. If the wind speed is specified, then the mean square height of the surface may be obtained. This is

$$\sigma^2 = c \frac{\pi}{2} \sqrt{\frac{\pi}{2}}\, 3 \left(\frac{s}{2g}\right)^5$$

Thus for the Neumann-Pierson spectrum, the mean square height is proportional to the 5th power of the wind speed. It should be noted that although we have separated the equation for $\langle f_1 f_2^* \rangle$ into coherent and incoherent components, the computer program will add the two factors together with the corresponding constants. To find the complex degree of coherence, it is necessary to evaluate $\langle p_1 p_1^* \rangle$ and $\langle p_2 p_2^* \rangle$. $\langle p_1 p_1^* \rangle$ is obtained by setting $a_2=a_1$, $b_2=b_1$ and $c_2=c_1$. For example from equation #20, we obtain

$$\langle p_1 p_1^* \rangle_{C\phi H} = k_1 (2\pi L^2)^2 \exp\left[-\frac{k^2 L^2}{2}(2a_1^2 + 2b_1^2)\right]$$

The computer program for the computation of the complex degree of coherence is given in Appendix A.

RESULTS

For our computations, we have chosen a frequency of 400 Hz and an angle of incidence of 45°. The incident and reflected ray are coplanar with the normal to the surface at the origin. One of the reflected directions was fixed at $\theta=45^\circ$. (See Figure #2).

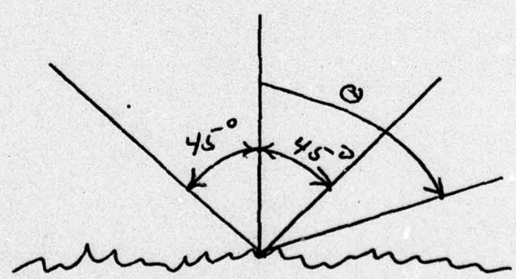

Fig. 2

The other direction was varied in $.1^\circ$ increments from 41° to 49°. The wind speed was held fixed for each computer run. In Figure #3, 3 computer runs are shown for wind speeds of 5, 7.5 and 10 knots. As stated previously, θ represents the direction of the second reflected ray. Since the first ray is fixed at 45°, when the second ray is at 45°, a complex degree of coherence of 1 is obtained, by definition. All 3 curves are thus correct at $\theta=45^\circ$. All 3 curves show perfect coherence for θ close to 45° and all 3 curves are zero when θ is $\pm 2^\circ$ from 45°. Physically, the ray in the specular direction has a coherent component which is high at low wind speeds. The coherent component decreases as θ goes further away from the specular direction. The coherence between the two rays is due to the coherence between the two coherent components. However, the coherent component is almost 0 when the direction is outside of the beamwidth (BW) of the insonified region. (See Nuttall and Cron[3], Equation #7) For an $L=32\lambda$, such as chosen in these computations,

$$BW \simeq \frac{\lambda}{L}\frac{180}{\pi} \text{ degrees} = \frac{\lambda}{32\lambda}\frac{180}{\pi} = 1.79^{\circ}$$

Thus the BW is on the order of 2°.

As L is increased, the coherent region decreases. It should be noted that in the farfield, a coherence on the order of a few degrees may represent a large linear region of coherence along an array. 5 knots represents a smoother surface than 7.5 or 10 knots and thus has a larger region of coherency.

Some of the parameters associated with the case shown in Fig. 3 are tabulated in Table I.

Speed in Knots	σ in cms	$\beta = kc\sigma$	$\beta_{12} = k^2\sigma^2 C_1 C_2$
2	.27	.0062	.000039
5	2.6	.0617	.0038
7.5	7.28	.1699	.0289
10	14.95	.3488	.1216
15	41.21	.9611	.9503

Note that the wind speed of 15 knots has a β_{12} that is close to 1 and therefore does not fall into the category of small roughness. For a wind speed of 2 knots, the surface is almost like a smooth mirror and computation shows a coherence of 1 from 41° to 49°. It is probably perfectly coherent in all regions.

Fig. 4 represents the case of one position fixed at the nonspecular direction of 55°. For this case it was found that as the wind speed changed from 2 to 10 knots, the curves did not change much.

The coherency drops much faster for this case then for the specular direction. Fig. 5, represents the case of one position being held at 65°. The difference between the 2 knot case and the 10 knot case is hard to distinguish on the plot. An investigation of the parameters shows that both curves are dependent on the tails of the surface wave height spectrum. However, the tails of the wave height spectrum are very close to one another at high surface frequencies.

CONCLUSION

A model and equations have been obtained for the spatial coherence in the far-field for a signal reflected from a time varying random surface. Computations and plots of values for specific cases have been presented. Only the low roughness case has been presented.

Plans are being made to obtain the incoherent component of spatial coherence for arbitrary roughness. The Fresnel region case is also being considered. In addition to this, experimental data of elements of an array have been obtained and will be analyzed in the near future.

ACKNOWLEDGEMENT:

The writer thanks Dr. A. Nuttall for discussions on this study and to Dr. W. Marsh and Dr. A. Nuttall on discussions on the symmetry properties of the spatial coherence function.

Benjamin F. Cron
BENJAMIN F. CRON
Research Associate

REFERENCES

1. B. F. Parkins, "Coherence of Acoustic Signals Reradiated from the Time-Varying Surface of the Ocean", Journal of the Acoustical Society of America, Vol 45, No 1, January 1969.

2. C. Eckart, "The Scattering of Sound from the Sea Surface", Journal of the Acoustical Society of America, Vol 25, No 3, May 1953.

3. A. Nuttall and B. Cron, "Spectrum of a Signal Reflected from a Time-Varying Random Surface", NUSC-Report NL-3013 Aug 25, 1970.

4. M. Born and E. Wolf, "Principles of Optics", Pergamon Press, London (1959)

5. B. Kinsman, "Wind Waves", Prentice-Hall Inc., New York (1965)

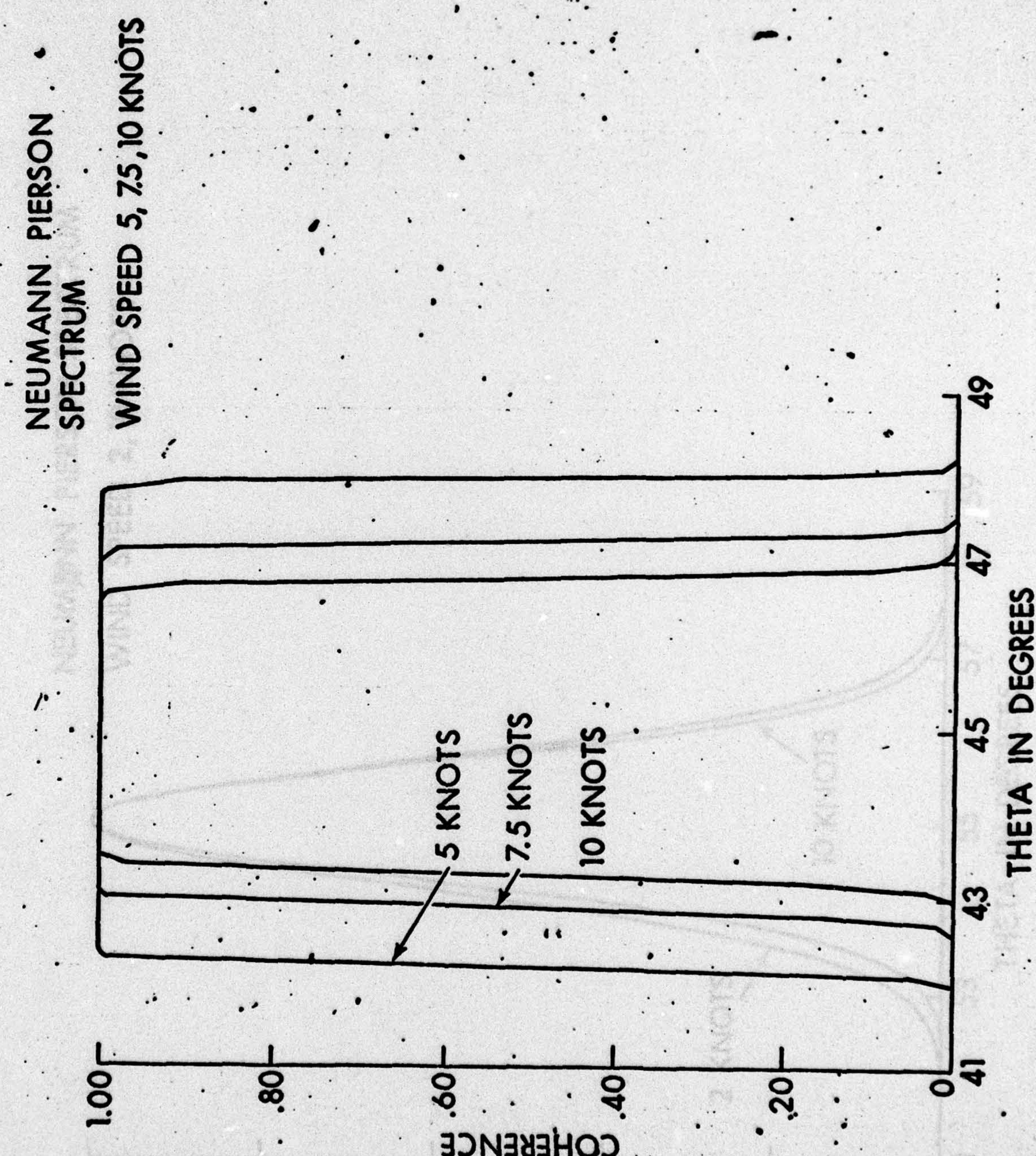
NEUMANN PIERSON SPECTRUM
WIND SPEED 5, 7.5, 10 KNOTS
5 KNOTS
7.5 KNOTS
10 KNOTS
COHERENCE
1.00
.80
.60
.40
.20
0
41
43
45
47
49
THETA IN DEGREES

FIGURE 3

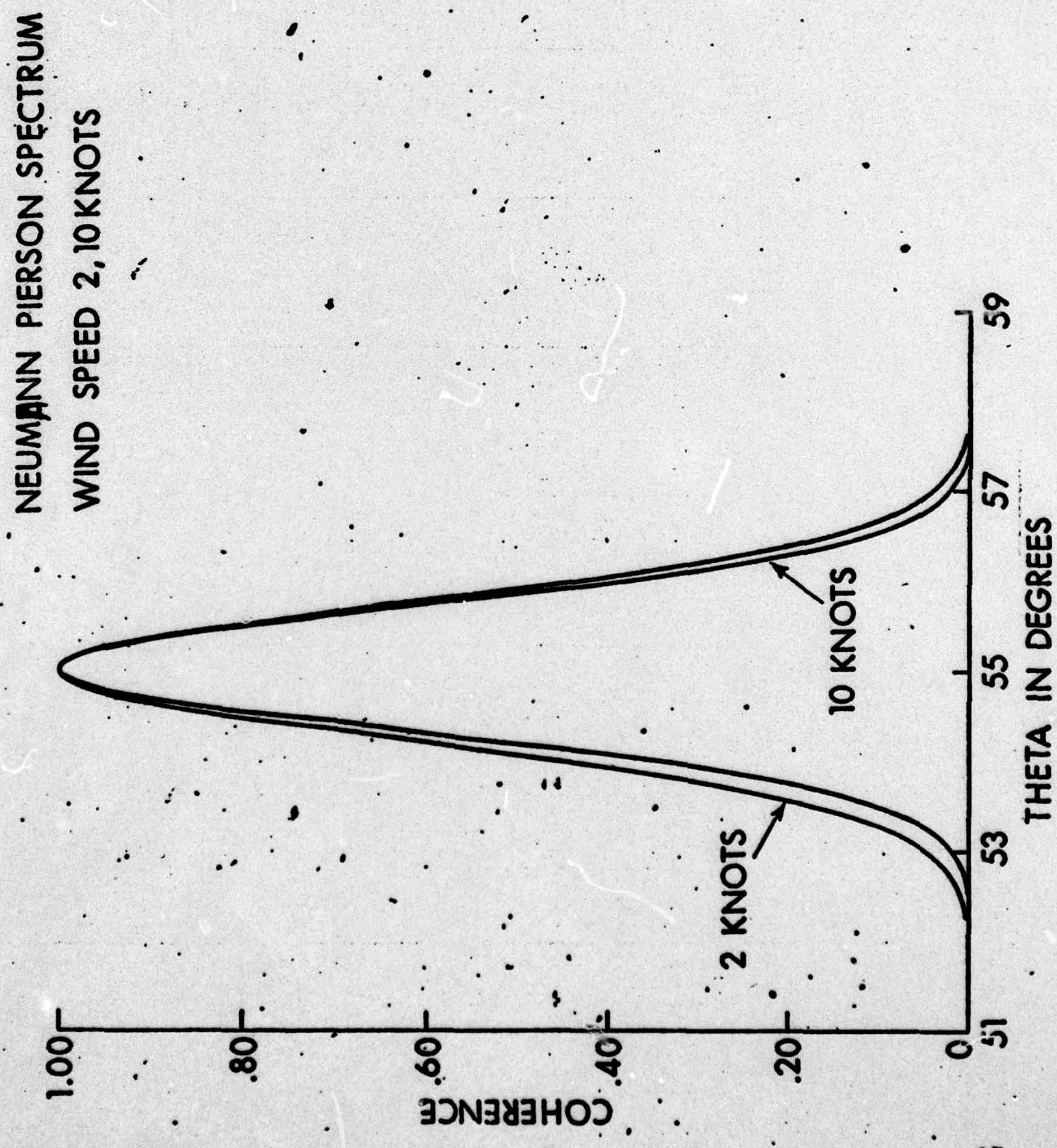
NEUMANN PIERSON SPECTRUM
WIND SPEED 2, 10 KNOTS
COHERENCE
1.00
.80
.60
.40
.20
0
51
53
55
57
59
THETA IN DEGREES
2 KNOTS
10 KNOTS

FIGURE 4

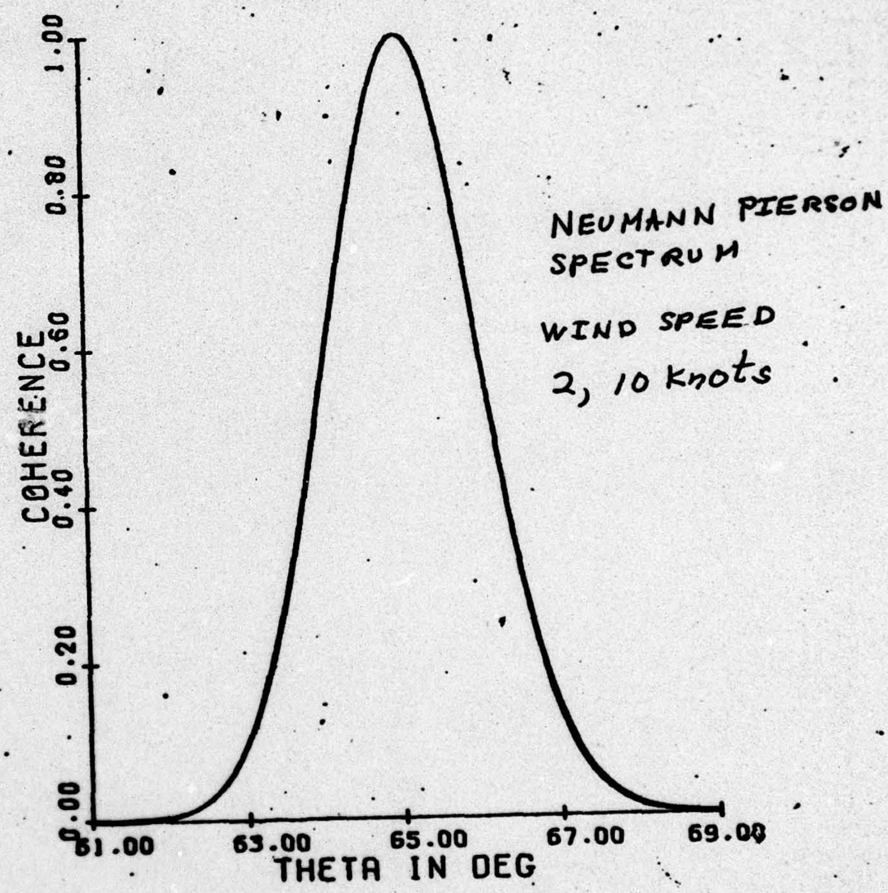
1.00
0.80
0.60
0.40
0.20
0.00
COHERENCE
61.00
63.00
65.00
67.00
69.00
THETA IN DEG
NEUMANN PIERSON SPECTRUM
WIND SPEED
2, 10 knots

FIGURE 5

APPENDIX A

COMPUTER PROGRAM

```
      PARAMETER NP=080,NP1=NP+1,NT=NP+1,N1=NP+2,N2=NP+3
      REAL X1(N2),Y1(N2),BUFFER(10000)
      IMPLICIT DOUBLE PRECISION(A-H,O-Z)
      DIMENSION CO(NP1)
   31 FORMAT(5D6.1,D9.4,D5.0)
   33 FORMAT(1X,6D16.8/6D16.8/6D16.8//)
      DEFINE F4(X,Y)=SQRT(SQRT(X*X+Y*Y))
      SPMT=50.9D0
      SP=51.D0
      CALL PLOTS(BUFFER,10000,6)
      CALL PLOT(0,0,100)
      CALL PLOT(0.,0.,-3)
      CCM=30.48D0
      CFM=30500.D0
      G=980.665D0
      C=5000.D0
      C=C*CCM
      F=400.D0
      PI=3.14159265358979324D0
      AMDA=C/F
      WN=2.*PI/AMDA
      WN2=WN*WN
      CF=PI/180.D0
   30 READ(3,31,END=32)TI,HI,TS1,HS1,HS2,SK,PL
      PL=PL*C/F
      PL2=PL*PL
      GNF=2.*PI*PL2
      GNF=GNF*GNF
      S=SK*185200.D0/3600.D0
      S2=S*S
      SC=S/(2.*G)
      SC2=SC*SC
      SC4=SC2*SC2
      SC5=SC4*SC
      PID2=PI/2.
```

```
      SPID2=SQRT(PID2)
      VAR=CFM*PID2*SPID2*3.D0*SC5
      SIG=SQRT(VAR)
      DO 26 NTS2=1,NP1
      TS2=NTS2*.1D0+SPMT
      TS2R=TS2*CF
      TIR=TI*CF
      HIR=HI*CF
      TS1R=TS1*CF
      HS1R=HS1*CF
      HS2R=HS2*CF
      AI=SIN(TIR)*COS(HIR)
      BI=SIN(TIR)*SIN(HIR)
      CI=COS(TIR)
      AS1=SIN(TS1R)*COS(HS1R)
      BS1=SIN(TS1R)*SIN(HS1R)
      CS1=COS(TS1R)
      AS2=SIN(TS2R)*COS(HS2R)
      BS2=SIN(TS2R)*SIN(HS2R)
      CS2=COS(TS2R)
       A1=AI+AS1
       B1=BI+BS1
       C1=CI+CS1
       A2=AI+AS2
       B2=BI+BS2
       C2=CI+CS2
       AS=(A1+A2)/2.
       BS=(B1+B2)/2.
       ARGA1=WN*A1*PL
       ARGA2=WN*A2*PL
       ARGB1=WN*B1*PL
       ARGB2=WN*B2*PL
       ARGDA=WN*PL*(A1-A2)
       ARGDB=WN*PL*(B1-B2)
       ARDA2=ARGDA*ARGDA
```

```
      ARDB2=ARGDB*ARGDB
      SA1=EXP(-ARGA1*ARGA1/2.)
      SB1=EXP(-ARGB1*ARGB1/2.)
      SA2=EXP(-ARGA2*ARGA2/2.)
      SB2=EXP(-ARGB2*ARGB2/2.)
      CC=SA1*SA2*SB1*SB2
      CC=CC*GNF
   18 OMEG=SQRT(G*WN)*F4(A1,B1)
      IF(OMEG)19,20,19
   19 A10M=CFM*EXP(-2.*G*G/(OMEG*OMEG*S2))
      A10M=A10M/(OMEG**6)
      CINF=SQRT(WN*G)*(PI**3)*PL2*2.
      CIN=CINF*C1*C2*EXP(-ARDA2/4.)*EXP(-ARDB2/4.)
      OM12=SQRT(G*WN)*F4(AS,BS)
      OM122=OM12**2
      A12M=CFM*EXP(-2.*G*G/(OM122*S2))
      A12M=A12M/(OM12**6)
      F12=F4(AS,BS)**3
      GO TO 21
   20 CIN=0.
   21 SA12=SA1*SA1
      SB12=SB1*SB1
      SA22=SA2*SA2
      SB22=SB2*SB2
      C11=SA12*SB12
      C11=C11*GNF
      C22=SA22*SB22
      C22=C22*GNF
      F11=(F4(A1,B1))**3
      IF(F4(A1,B1))51,50,51
   51 CI11=CINF*C1*C1*A10M/F11
      GO TO 52
   50 CI11=0.
   52 OMEG2=SQRT(WN*G)*F4(A2,B2)
      IF(OMEG2)23,24,23
```

```
   23 OMEG22=OMEG2*OMEG2
      A20M=CFM*EXP(-2.*G*G/(OMEG22*S2))
      A20M=A20M/(OMEG2**6)
      F22=(F4(A2,B2))**3
      CIN=CIN*A12M/F12
      GXY=CC+CIN
      CI22=CINF*C2*C2*A20M/F22
      GO TO 25
   24 CI22=0.
   25 GXX=C11+CI11
      GYY=C22+CI22
      CDEN=SQRT(GXX)*SQRT(GYY)
      COH=GXY/CDEN
      CO(NTS2)=ABS(COH)
      BET=WN*C1*SIG
      BET12=WN2*C1*C2*VAR
      WRITE(4,33)SK,SIG,BET,BET12,TS2,COH
   26 CONTINUE
      DO 40 NTS2=1,NP1
      X1(NTS2)=NTS2*.1D0+SPMT
      Y1(NTS2)=CO(NTS2)
   40 CONTINUE
      X1(N1)=SP
      X1(N2)=2.
      Y1(N1)=0.
      Y1(N2)=.2
      CALL LINE(X1,Y1,NT,1,0,0)
      GO TO 30
   32 CALL AXIS(0.,0.,12HTHETA IN DEG,-12,4.,0.,X1(N1),X1(N2),10.).
      CALL AXIS(0.,0.,9HCOHERENCE,+9,05.,90.,Y1(N1),Y1(N2),10.)
      CALL PLOT(20.,0.,-3)
      CALL PLOT (0.,0.,993)
      STOP
      END
```